Journal of Applied Pharmaceutical Science Vol. 8(03), pp. 014-022, March, 2018
Available online at http://www.japsonline.com
DOI: 10.7324/JAPS.2018.8303
ISSN 2231-3354


# Molecular docking study on the interaction between 2-substituted-4,5-difuryl Imidazoles with different Protein Target for antileishmanial activity

Julio Alberto Rojas Vargas[1], America García Lopez[1], Mariana Castro Piñol[2], Matheus Froeyen[3*]

[1]Chemistry Department, Natural Science Faculty, Universidad de Oriente, Santiago de Cuba, Cuba.
[2]Oriente Pharmaceutical Lab Santiago, BIOCUBAFARMA group, Santiago de Cuba, Cuba.
[3]Medicinal Chemistry, Department of Pharmacy, Rega Institute, KU Leuven, Leuven, Belgium.

**ARTICLE INFO**

Article history:
Received on: 08/11/2017
Accepted on: 12/01/2018
Available online: 30/03/2018

***Key words:***
Antileishmanial activity, Leishmania, Molecular docking, 2-substituted-4,5-difuryl imidazoles, *Leishmania arginase, Leishmania trypanothione synthetase amidase, Leishmania trypanothione reductase*.

**ABSTRACT**

Leishmaniasis is a disease which is caused by the protozoa Leishmania and is considered the second-highest cause of death worldwide by parasitic infection. Looking for the right chemotherapy against leishmaniases has been difficult because of the high toxicity of the most effective drugs. Computational Chemistry plays an important role in the research of new possible medicines. In this work, docking analysis was carried out to study the effects of nine 2-substituted-4,5-difuryl Imidazole on *Leishmania arginase, Leishmania trypanothione synthetase amidase* and *Leishmania trypanothione reductase* and results were compared with three known drugs, and with targets potential inhibitors. ΔG, Ki and binding interactions in the targets active sites were reported. Results show that 4, 5-di (furan-2-yl)-2-(5-(4-nitrophenyl) furan-2-yl)-1H imidazole and 4-(5-(4,5-di(furan-2-yl)-1H-imidazol-2-yl) furan-2-yl) benzoic acid are promising leads, so the study of these compounds is recommended.

## INTRODUCTION

Leishmanisis is located within the thirteen tropical diseases more neglected (WHO, 2016), caused by over twenty different species of *Leishmania* parasite (e.g., *L. donovoni*, *L. infantum*, *L. major*, *L. mexicana*, etc.), we can find it in three clinical form: cutaneous (*L. major, L. tropica* and *L. mexicana*), mucocutaneous (*L. braziliensis*) and visceral (*L. donovani* and *L. infantum*) (Loría and Andrade, 2014; Reithinger *et al.,* 2007). The diseases is transmitted by infected female Phlebotomine sandfly, a dipteran, which transmits the parasite to human during blood sucking (Myler and Fasel, 2008). This malady is endemic from of Central and South American countries (Tempone *et al.*, 2005).

Due to its characteristics of opportunistic pathogen has generated great interest in the scientific community the need to control it. The proven treatment for Leishmanisis include the antimonials sodium stibogluconate (pentostam) and meglumine antimoniate (glucantime), but the adverse side effects associated with these compounds and drug resistance is emerging. However, alternative antileishmanial chemotherapies include the compounds amphotericin B and pentamidine, which are generally more toxic than the pentavalent antimonials (Arboleda *et al.*, 2013; Sundar and Rai, 2002).

So far, others drugs are used as replacement of these drugs, in some cases of uncertainly effective therapy such as allopurinol, the AmBisome® (formulation of amphotericin B in

*Corresponding Author
*Matheus Froeyen; Medicinal Chemistry, Department of Pharmacy, Rega Institute, KU Leuven, Leuven, Belgium.*
*E-mail: mathy.froeyen @ kuleuven.be*

liposomes) and ketoconazole (Jebran *et al*., 2014).

Nowadays, have grown the indentification of specific biological targets by the use of computational tools for the desing of new drugs with the aim to decreased illness. Within commnon tools used with this objective we can found the molecular docking and molecular dynamic, commonly used for elucidation of leishmaniasis targets and find out the interaction and dynamics of drugs and target at molecular level (Peitsch and Schwede, 2000).

Imidazoles are an important group heterocycles that contain nitrogen and are currently under intensive studie due to their broad range of applications (Gharib *et al*., 2014) such as angiotensin inhibitors (Trujillo *et al*., 2009), anti-inflammatory (Palkowitz *et al*., 1994), glucagon antagonist (Chang *et al*., 2001), antiviral (Sharma *et al*., 2009), fungicidal, (Laufer and Koch, 2008; Kumar *et al*., 2003), and high cytotoxicity, which has indicated them as new candidates in cancer therapy (King *et al*., 2006). Compounds containing imidazole moiety have many pharmacological properties and play important roles in biochemical processes (Lambardino and Wiseman, 1974). The potency of the imidazoles can be attributed to its hydrogen bond donor-acceptor capability as well as its high affinity for metals (e.g., Zn, Fe, Mg), which are found in many protein active sites (Takle *et al*., 2006). Substituted imidazoles have been reported to possess anti-mycobacterial, antimicrobial, anthelmintic, anti-inflammatory, anticonvulsant and insecticidal properties (Kumar *et al*., 2008; Manal *et al*., 2014; Safari *et al*., 2013). Many studies showed that azole heterocycles such as imidazole and triazole are useful pharmacophores for anti-mycobacterial activity (Zampieri, 2009; Chauhan *et al*., 2010).

In the present study, the structural models of 2-substituted-4,5-difuryl Imidazoles in the *Trypanothione Synthetase* (***TSy***), *Trypanothione Reductase* (***TRe***) and *Arginase I* (***ArgI***) binding sites have been created, which may facilitate further development of more potent antileishmanial agents. The overall scores were used to choose the final models. Protein-ligand dockings were performed between the molecular model of *L. infantum* ***TRe***, *L. major* ***TSy*** and *L. amazonensis* ***ArgI*** and 2-substituted-4,5-difuryl Imidazoles. The analyses *in-silico* of probable inhibition and interaction models is not conclusive report on the antileishmanial activity of 2-substituted-4,5-difuryl Imidazoles, but will be useful to design molecules that may have antileishmanial activity.

## MATERIALS AND METHODS

### Computational Resource

Molecular modelling was performed using the High-performance computing capabilities of the Cluster of Chemistry Department of University of Oriente running the Linux operating system Debian 7.0 distribution.

### Ligands and Proteins Preparation for Docking

Autodock is a very popular open source docking program. The pdb file was prepared using the software UCSF Chimera molecular graphic system, version 1.10.227. The following target proteins with their Protein Data Bank (PDB) ID were selected, Trypanothione Reductase from *Leishmania Infantum* – PDB ID: 2JK6 (**TRe**), Trypanothione Synthetase from *Leishmania major* – PDB ID: 2VOB (**TSy**) and Arginase I from *Leishmania amazonensis* - PDB ID: 1T5F (**ArgI**). The different protein structures contain identical domains, for these proteins we used chain A for each protein. Finally, the resulting prepared 3D structure of the proteins was saved as PDB file. Using AutodockTools 1.5.6 (ADT) (Sanner, 1999), Kollman united atom charges, solvation parameters and polar hydrogens were added to the protein for the preparation of the enzyme in the docking simulations. Since the ligands are not peptides, Gasteiger charges were assigned and non-polar hydrogens were merged.

ChemBioDraw (Evans, 2014) was used to draw the structures of 2-substituted-4,5-difuryl Imidazoles (Figure 1) and designed taking into account reference (Speck *et al*., 2011). ChemBio3D Ultra 12.0 (Evans, 2014) was used to optimize the geometry, running a MMFF94 energy minimization of the 3D structures. The Gasteiger (Gasteiger and Marsili, 1980) charge calculation method was used and partial charges were added to the ligand atoms before docking.

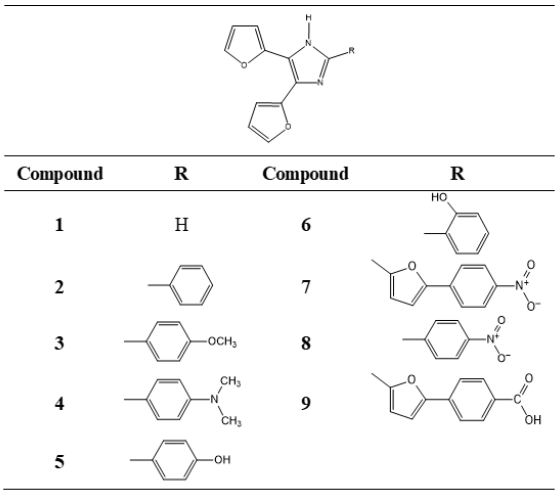


**Fig. 1:** Chemical structure of 2-substituted-4,5-difuryl Imidazole.

### Identification of binding site residues

The binding site residues for ***ArgI***, ***TSy***, and ***TRe*** from *Leishmania amazoenesis* were identified from the analysis of the Arginase I-AOH complex – PDB ID: 1T5F (Shin *et al*., 2004), Trypanothione Synthetase – PDB ID: 2VOB (Fyfe *et al*., 2008) from *Leishmania major* and Structure of Trypanothione Reductase from *Leishmania infantum* – PDB ID: 2JK6 (Baiocco, 2009).

### Grid box preparation and docking

Docking experiment were performed between 2-substituted-4,5-difuryl Imidazoles and different targets of Leishmania. AutoDock requires pre-calculated grid maps, one for each atom type, present in the ligand being docked. This grid stores the potential energy arising from the interaction with the macromolecule and must surround the region of interest (active site) in the macromolecule. Grid box parameters (Table 1) were set by using ADT. The molecular docking program AutoDock (version 4.2) (Sanner, 1999) was employed to perform the docking experiment.

**Table 1:** Grid box parameters selected for the target enzymes.

| PDB ID (Resolution) | Name | Enzyme | Coordinates of center of box | Size (points) | Spacing (Å) |
|---|---|---|---|---|---|
| 2VOB (2,3 Å) | TSy | Trypanothione Synthetase | x: −5.339 y: −21.67 z: 8.498 | 60 × 60 × 60 | 0.375 |
| 2JK6 (2,95 Å) | TRe | Trypanothione Reductase | x: 30.449 y: 47.483 z: −4.312 | 60 × 60 × 60 | 0.375 |
| 1T5F (2,2 Å) | ArgI | Arginase-I | x: 24.748 y: 12.201 z: 8.961 | 60 × 60 × 60 | 0.375 |

The Lamarckian Genetic Algorithm was used to explore the best conformational space for the ligand with a 50 docking runs for each ligand. The maximum numbers of generation and evaluation were set at 27000 and 2500000, respectively. Other parameters were set as default. After complete execution of Autodock fifty conformations of the ligands in complex with the receptor were obtained, which were ranked based on binding energy and inhibition constant (Ki).

Docking calculations can be validated by redocking ligands that were cocrystallized in the receptor structures (Arba *et al.*, 2017). However in our target structures, no inhibitors were present, so we opted for validation by docking some known antimicrobial drugs as Ketoconazole, Pentamidine and Miltefosine taken from DrugBank (Wishart *et al.*, 2006). They were built and docked (Figure 2).

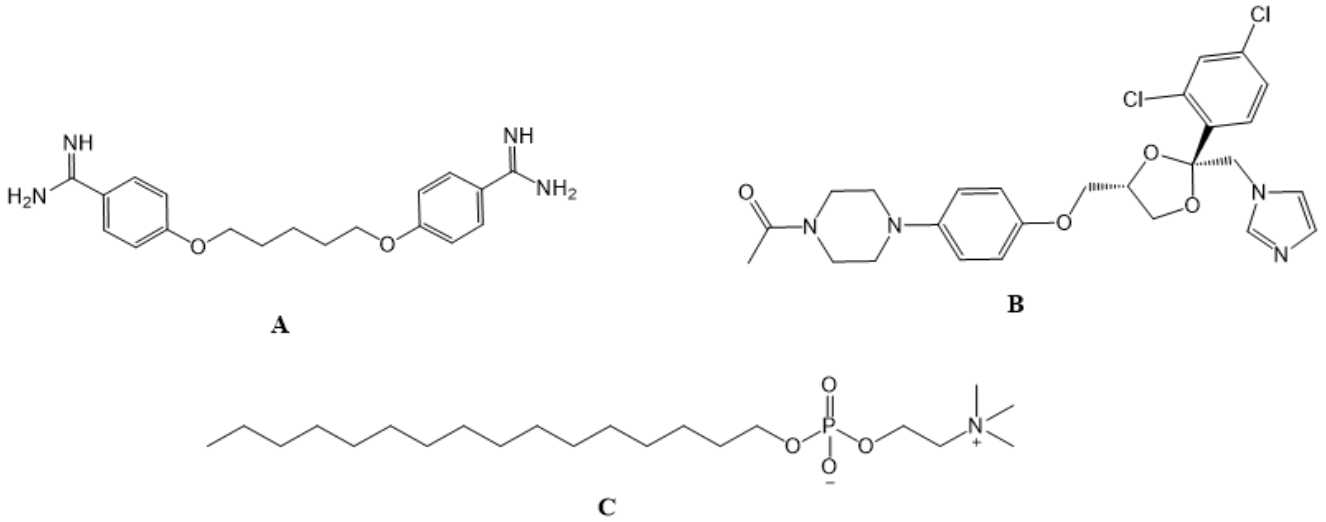


**Fig. 2:** Structure of control compounds Pentamidine (A), Ketoconazole (B) and Miltefosine (C).

## RESULTS AND DISCUSSION

Molecular docking studies of nine 2-substituted-4,5-difuryl Imidazoles (Figure 1) were carried out with three protein Trypanothione Reductase (**TRe**), Trypanothione Synthetase (**TSy**) and Arginase-I (**ArgI**) from the *Leishmania infantum*, *Leishmania major* and *Leishmania amazoenesis* parasite respectively, using Autodock 4.2, to identify the binding mode of ligands and the intermolecular interaction between ligands and different target proteins.

The poses docked for each of the compounds were evaluated and the pose with the lowest binding free energy and the inhibition constant was thereby chosen (Table 2).

**Table 2:** Predicted binding free energies and inhibition constant observed between the compounds and the target enzymes.

| Ligand | Enzymes | | | | | |
|---|---|---|---|---|---|---|
| | *TRe 2JK6* | | *TSy 2VOB* | | *ArgI 1T5F* | |
| | ΔG (kcal/mol) | Ki (μM) | ΔG (kcal/mol) | Ki (μM) | ΔG (kcal/mol) | Ki (μM) |
| 1 | −6.39 | 20.9 | −6.06 | 35.9 | −6.38 | 52.7 |
| 2 | −8.36 | 0.75 | −8.13 | 1.11 | −6.07 | 36.9 |
| *3* | −8.01 | 1.35 | −8.28 | 0.85 | −6.48 | 17.9 |
| 4 | −6.71 | 12.2 | −8.32 | 0.79 | −5.86 | 51.0 |
| 5 | −8.05 | 1.25 | −8.05 | 1.26 | −6.55 | 15.7 |
| 6 | −8.08 | 1.19 | −8.68 | 0.44 | −6.34 | 22.4 |
| 7 | −9.12 | 0.21 | −10.5 | 0.02 | −7.47 | 3.34 |
| 8 | −7.17 | 5.59 | −8.57 | 0.52 | −6.18 | 29.5 |
| 9 | −9.33 | 0.14 | −10.1 | 0.04 | −6.91 | 8.65 |

The lowest binding free energy (i.e. best docking score) and inhibition constant indicated the highest ligand/protein affinity.

The docking studies were done in comparison with control compounds. As control compounds were used Ketoconazole, Pentamidine and Miltefosine (Figure 2), these drugs are used currently against the Leishmania parasites (Rodrigues *et al.*, 2012; Alam *et al.*, 2012).

The predicted binding free energy observed for ligand **7** was for **TRe** −9,12 kcal/mol, **TSy** −10.5 kcal/mol and ***ArgI*** −7.47 kcal/mol; ligand **9** binding is stabilized by −9.33 kcal/mol to **TRe**, −10.1 kcal/mol to **TSy** and −6.91 to **ArgI**. The inhibition constant value for ligand **7** and **9** result in very similar values, 0,21 and 0,18 µM for **TRe**, 0,02 and 0,04 µM for **TSy** and 3,34 and 8,65 µM for **ArgI**, respectively.

When the chemical structure of **7** and **9** (Figure 3) was compared, it was observed that both ligands possess two furyl rings joined to the imidazole ring, and also a furylphenyl group. The existence of these aromatic rings at the same position increases the length of the chain, the number of bond torsions and the accessibility of heteroatoms and substitutions from the amino acids residues of the enzyme in the active site. Therefore, an important number of hydrophobic interaction and hydrogen bonds exist that stabilize the enzyme-ligand complex.

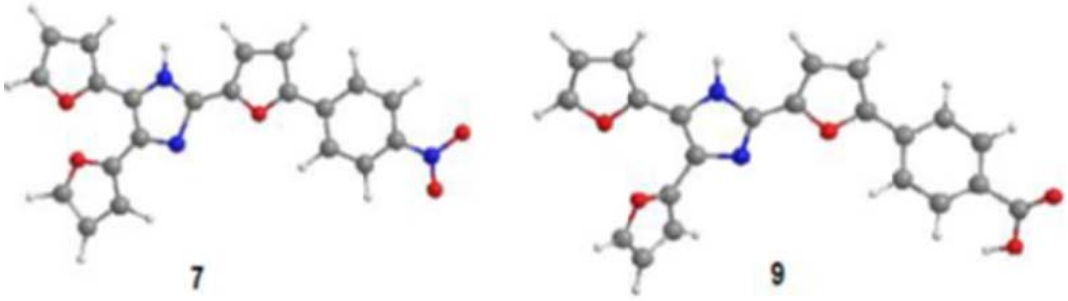


**Fig. 3:** Structure chemical three-dimensional of ligand **7** and **9**.

### *L. infantum* TRe

Compound **7** was found (Table 3) to establish hydrogen bonds with [O….H-N] Gly15, [N….H-N] Thr335 and [O….H-N] Thr335 with a distance of 2,90, 3,09 and 3.33 Å, respectively (Figure 4B), and hydrophobic interaction with Ala365, Cys52, Cys364, Leu334, Pro336, Ser14, Tyr198 and Thr51 (Figure 4B) residues of TRe. Also, it was observed that compound 9 (Table 3) interacts by hydrophobic interaction with Ala365, Ala338, Cys57, Cys364, Pro336 and Leu334 residues of TRe, also were found hydrogen bonds with [O….H-N]Asp327, [O….H-N] Gly15, [O….H-N]Thr335 and [N….H-O]Tyr198, with a distance of 3.03 Å for [O….H-N]Asp327 and [O….H-N]Gly15, 3.00 Å for [O….H-N]Thr335 and 3.27 Å [N….H-O]Tyr198 (Figure 4A). Both compounds (**7** and **9**) share the residues Cys52, Cys57 and Thr335 involved in the active site of TRe (Baiocco *et al*., 2009).

**Table 3:** Interactions observed between compounds **7** and **9** and the different target enzymes.

| Enzyme | Imidazole | Residues making hydrophobic contacts | H-bond/Coordination Interactions |
|---|---|---|---|
| TRe (2JK6) | **7** | Ala365, Cys52, Cys364, Leu334, Pro336, Ser14, Tyr198, Thr51, Asp327, Met333, Thr51, Ala338, Gly13 | Gly15 [N-H…. O], Thr335 [N-H….O], [N-H….N] Thr335 |
| | **9** | Ala365, Ala338, Cys57, Cys364, Pro336, Leu334, Ala338, Ser14, Gly326 | Asp327 [N-H….O], Gly15 [N-H….O], Thr335 [N-H….O], Tyr198 [O-H….N] |
| TSy (2VOB) | **7** | Arg613; Glu587; Glu614; Ile597; Tyr595; Phe333; Pro625; Lys590 | Ala596 [N-H…. O]; Ala596 [O-H….N] |
| | **9** | Glu614; Glu587; Ile 597; Lys 590; Pro 625; Tyr 595; Phe333 | Ala596 [N-H….O]; Ala596 [O-H….N]; Arg613 [N-H….O] |
| ArgI (1T5F) | **7** | Arg21; Cys19; Glu277; Gly142; His126; Pro20; Ser136; Thr135 | Asn279 [N-H….O]; Gly245[N-H….O]; Ser137 [O-H….N] |
| | **9** | Ala141; Arg21; Cys19; Glu277; Gly245; Pro20; Ser137; Val24 | Lys68 [N-H….O] |

### *L. major* TSy

On the other hand, compound 7 was found to interact by hydrophobic interactions with Ala596; Arg613; Glu587; Glu614; Ile597 and Tyr595 residues of TSy (Figure 5A), also it was observed for this compound to establish hydrogen bonds with Ala596 [N-H….O] and Ala596 [O-H….N] residues of TSy, with a distance of 2,70 Å and 3,33 Å respectively (Figure 5A). However, compound 9 showed hydrogen bond interactions with the same residues as in the compound 7 complex (Ala596 [N-H….O] and Ala596 [O-H….N]), and also with residue Arg613 [N-H….O] with a hydrogen bond distance of 3,21 Å (Figure 5B). The residue Arg613 is involved in the active site of TSy according to the reference (Barrett *et al*., 1999). Compound 9 showed hydrophobic interaction with Glu614, Glu587, Ile 597, Lys 590, Pro 625 and Tyr 595 residues.

### *L. amazonensis* ArgI

Compound 7 showed hydrogen bonds with Asn279 [N-H….O]; Gly245[N-H….O] and Ser137 [O-H….N] residues of **ArgI** (Figure 6A) and hydrophobic interactions with Arg21; Cys19; Glu277; Gly142; His126; Pro20; Ser136 and Thr135, some of those residues Arg21, Glu277 y His126 are involved in the active site according to reference (Kanyo *et al*., 1996). Also, it was observed that compound 9 interacts with Ala141; Arg21; Cys19; Glu277; Gly245; Pro20; Ser137 and Val24 residues of **ArgI** (Figure 6B) by hydrophobic interaction; as well it was found that compound 9 establishes a hydrogen bond with Lys68 [N-H….O] residue.

### Control inhibitors

The control inhibitors were docked under the same docking conditions against the enzymes **TRe**, **TSy** and **ArgI**. The docked poses for each control inhibitors were evaluated and the pose with the lowest binding free energy and the inhibition constant was thereby chosen. These results were compared with the better ligands **7** and **9** (Table 4).

**Table 4:** Comparison of predicted binding free energies and inhibition constant between the better ligands and control inhibitors.

| Ligand | Enzymes | | | | | |
|---|---|---|---|---|---|---|
| | *L. infantum TRe 2JK6* | | *L. major TSy 2VOB* | | *L. amazonenesis ArgI 1T5F* | |
| | ΔG (kcal/mol) | Ki (μM) | ΔG (kcal/mol) | Ki (μM) | ΔG (kcal/mol) | Ki (μM) |
| 7 | −9.12 | 0.210 | −10.5 | 0.020 | −7.47 | 3.34 |
| 9 | −9.20 | 0.179 | −10.1 | 0.040 | −6.91 | 8.65 |
| Ket.[a] | −9.77 | 0.068 | −9.81 | 0.064 | −7.68 | 2.34 |
| Pent.[b] | −8.57 | 0.526 | −8.71 | 0.410 | −6.91 | 8.57 |
| Milt.[c] | −4.72 | 345,9 | −5.47 | 97.10 | −4.87 | 271 |

a. Ketoconazole, b. Pentamidine, c. Miltefosine.

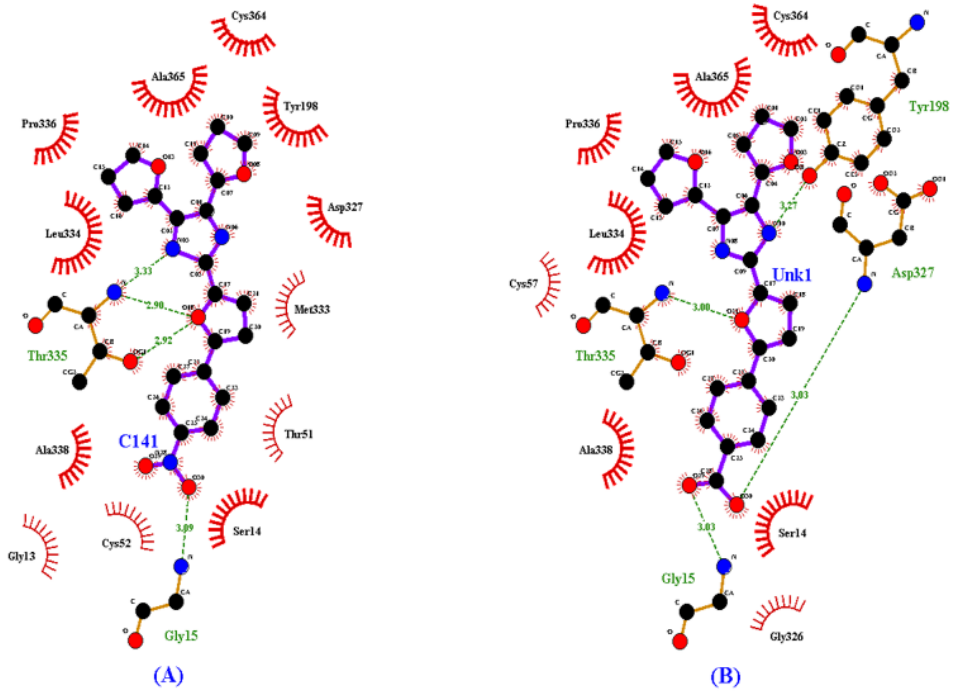


**Fig. 4:** Protein-ligand interaction 2D map of ligand **7** (A) and **9** (B) with ***TRe*** protein using Ligplot diagram (Wallace *et al*., 1996).

According to these results, both compounds **7** and **9** showed similar behavior against the enzymes **TRe**, **TSy** and **ArgI**, but compared with the control compounds, both ligands showed higher stability than the Pentamidine and Miltefosine drugs, only surpassed by the control Ketoconazole for the enzymes *L.infantum* **TRe** and *L. amazonenesis* **ArgI** (Table 4).

Ketoconazole showed an inhibition constant of 0,068 μM and a binding free energy of −9.77 kcal/mol; both values are similar to ligands **7** and **9** for **TRe** (Table 4). These similar values are due to similar structural conformation inside the enzyme **TRe** (Figure **7**). For *L. infantum* **TRe** the Ketoconazole interacted with Leu334, Pro336, Cys364, Ala363, Ala365, Thr335, Lys60, Phe367, Met333, Tyr198, Thr51, Cys57, Arg287, Ser162, Gly161 and Asp327 residues (Figure 7), in this case share following interacting residues with ligands **7** and **9**: Leu334, Pro336, Cys364, Cys57, Ala365 and Thr335; some of them involved in the active site of **TRe** (Baiocco *et al*., 2009).

The predicted binding free energies observed for Ketoconazole with *L. major* **TSy** was 9.81 kcal/mol, in this case ligands **7** and **9**, showed better values (Table 4) compared with this control drug. The residues Met251, Val263, Ser264, Phe626, Glu355, Ala627, Trp363, Ile612, Gln360, Cys356, Ala628, Arg613, Gly611, Gly599, Thr352 and Trp601 interacted with Ketoconazole (Figure 8). As we can observe in this figure, there exists a good superimposition between the ligand **7** and **9** with Ketoconazole inside the protein target *L. major* **TSy**.

For target **ArgI** the predicted free energies for Ketoconazole was −7.98 kcal/mol, with residues Cys19, Gly245, Pro20, Glu277, Ala141, Asn139, Thr246, Gly142, His126, Asp128, Glu186, Asp183, Asp181, Val182, Arg21 interacting with Ketoconazole (Figure 9). In this case ligands **7** and **9** share some interacting residues: Asp128, Asp183, Glu186, Asn130, Asp124, Glu277, His101, Asp232, Asp234 involved in the active site of ArgI (Figure 9) (Shin *et al.*, 2004). The superimposition inside the binding site of **ArgI** of ligand **7** and **9** with Ketoconazole is not good unlike in the case of proteins **TSy** and **TRe**.

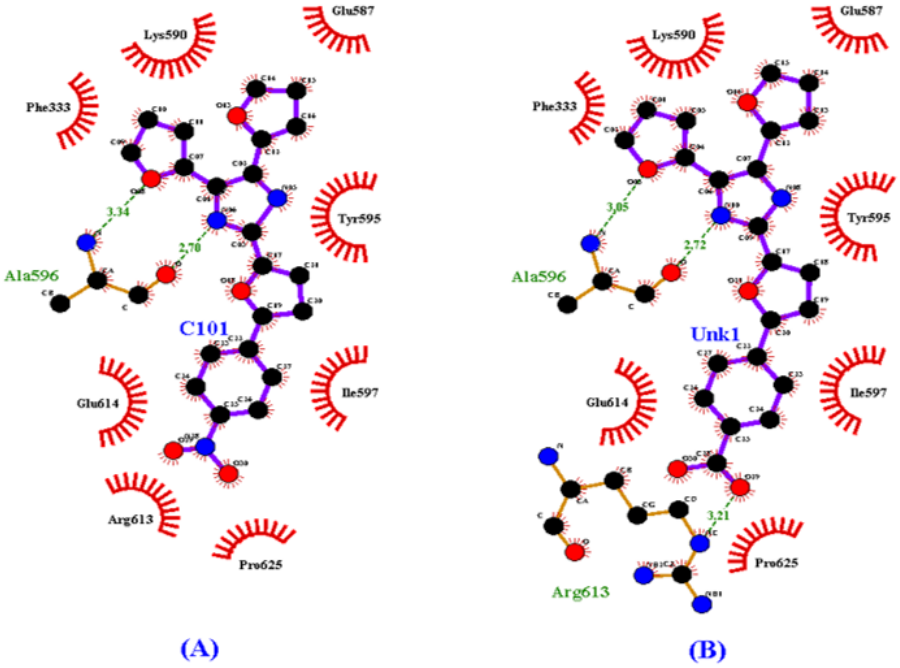


**Fig. 5:** Protein-ligand interaction 2D map of ligand **7** (A) and **9** (B) with ***TSy*** protein using Ligplot (Wallace *et al*., 1996).

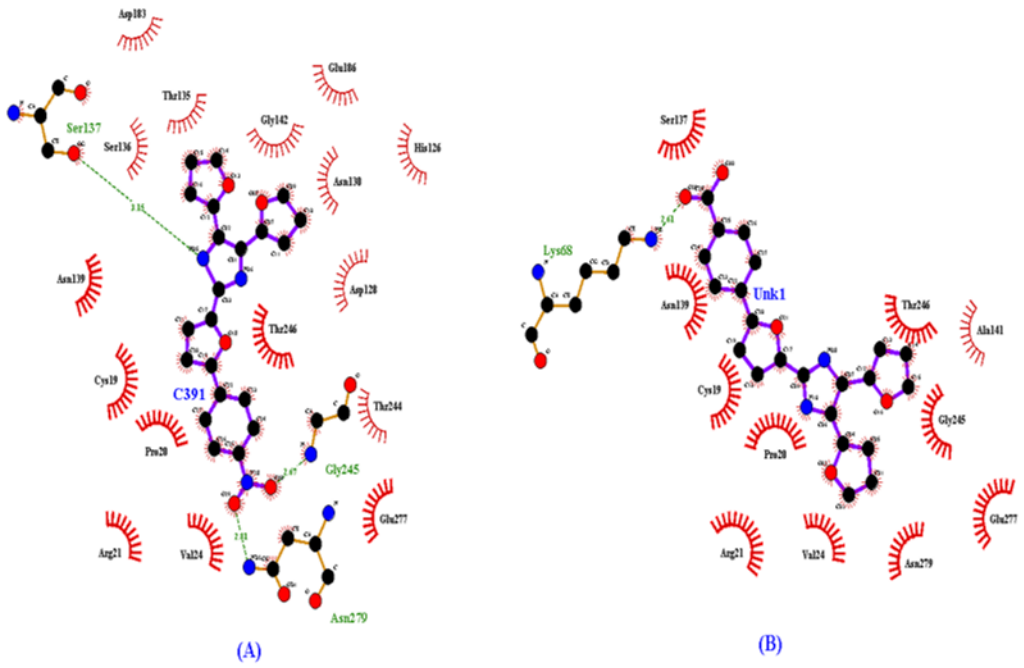


**Fig. 6:** Protein-ligand interaction 2D map of ligand **7** (A) and **9** (B) with ***ArgI*** protein using Ligplot (Wallace *et al*., 1996).

**Comparison with other molecular docking study in the same proteins**

In Table 5, we show published reports of molecular docking of possible inhibitory substances and the same target enzymes under study, under calculation conditions very similar to ours and compared with the data obtained in the present work of one of our potentially more active imidazoles. As shown in Table 5 in all cases, the values calculated for imidazole 2-[5-(4-nitrophenyl) furyl]-4,5-difurylimidazole (compound **7**) indicate greater stability in the coupling with the enzymes than the inhibitors reported by other authors.

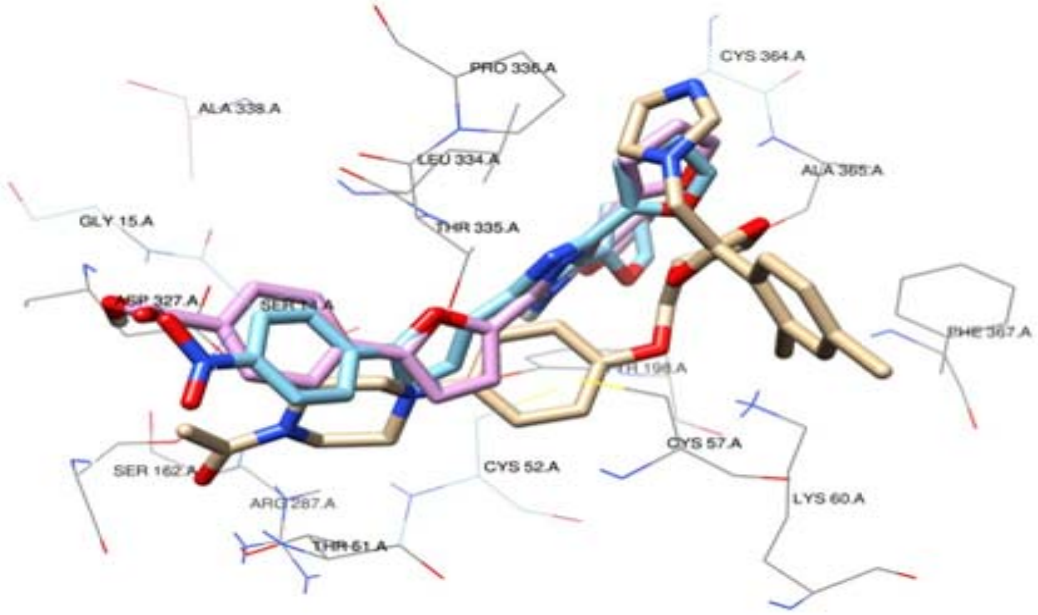


**Fig. 7:** Superimposition of control Ketoconazole (tan) with ligand **7** (sky blue) and **9** (orchid) against the enzyme *L. infantum* ***TRe***.

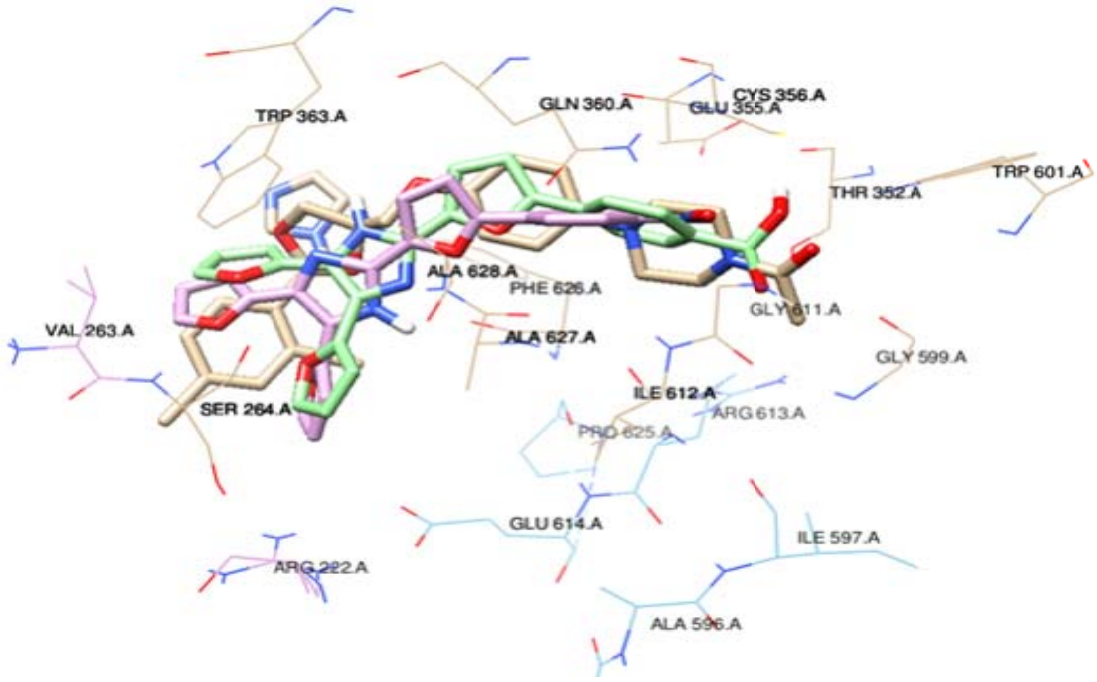


**Fig. 8:** Superimposition of control Ketoconazole (tan) with ligand **7** (orchid) and **9** (light green) against the enzyme *L. major* ***TSy***.

This assessment is analogous for the imidazole 2-[5-(4-carboxyphenyl)furyl]-4,5-difurylimidazole (compound **9**), even in some cases for other imidazoles studied which were not selected in this work as the most potentially active (see Table 2). The structures of the control inhibitors are markedly different from imidazoles (see Figures 2A, 2B), which explains the little coincidence in the interactions in the complexes formed by them with the corresponding enzymes and those found for 2-[5-(4-nitrophenyl)furyl]-4,5-difurylimidazole (compound **7**).

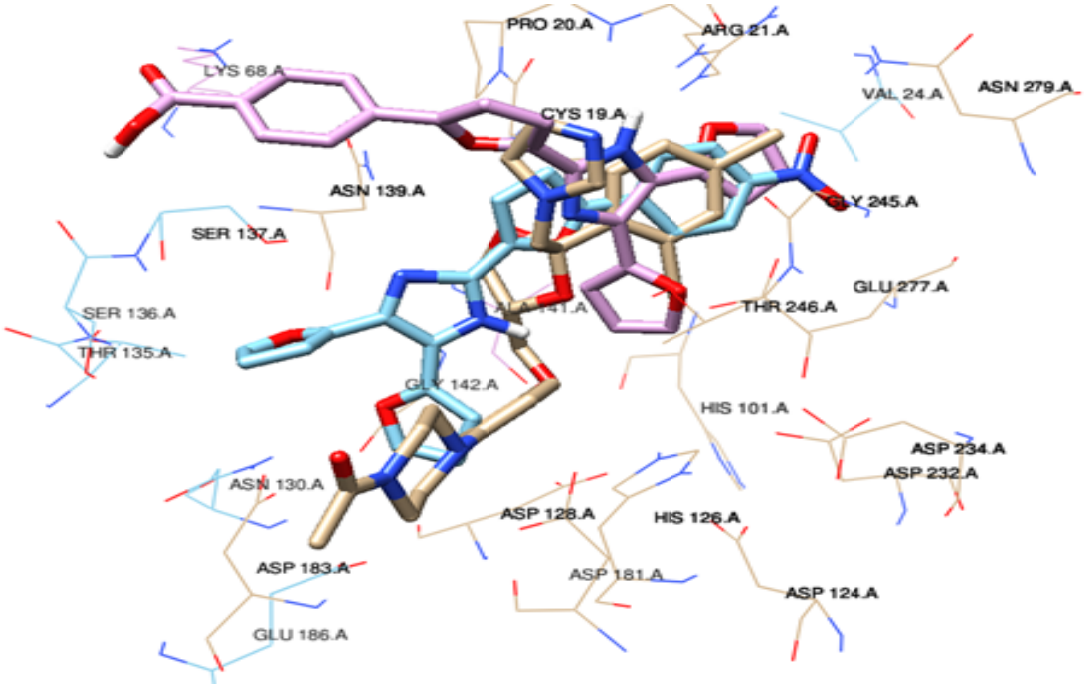


**Fig. 9:** Superimposition of control Ketoconazole (tan) with ligand **7** (sky blue) and **9** (orchid) against the enzyme *L. amazonensis* ***ArgI***.

**Table 5:** Comparison results of molecular docking reported by other authors with the better ligands (**7** and **9**) of this work.

| Ligand | Enzyme | Organism | ΔG (kcal/mol) | Ki (μM) |
|---|---|---|---|---|
| imidazole **7** | Arginase I | Leishmania amazonensis | −7.47 | 3.34 |
| imidazole **9** | | | −6.91 | 8.65 |
| (+)-catechin (dos Reis *et al*., 2013) | | | - | 12 |
| imidazole **7** | Trypanothione Synthetase-Amidase | Leishmania major | −10.5 | 0.02 |
| imidazole **9** | | | −10.1 | 0.04 |
| Sesquiterpene (Bernal and Coy-Barrera, 2014) | | | −8.9 | - |
| imidazole **7** | Trypanothione Reductase | Leishmania infantum | −9.12 | 0.21 |
| imidazole **9** | | | −9.33 | 0.14 |
| Taxifolin (Gundampati and Jagannadham, 2012) | | | −8.28 | 0.85 |
| Mangiferin (Gundampati *et al*, 2013) | | | −9.16 | 0.19 |

## CONCLUSIONS

The imidazoles studied 2-[5-(4-nitrophenyl)furyl]-4,5-difuryl-imidazole and 2-[5-(4-carboxyphenyl)furyl]-4,5-difuryl-imidazole better coupled with Arginase I, Trypanothione Synthetase-Amidase and Trypanothione Reductase taking into account the binding energies, the inhibition constant and the interactions with aminoacids residues in the active site. This stability is more remarkable with the enzymes Trypanothione Synthetase-Amidase and Trypanothione Reductase. These imidazoles have binding energy values than Milefosine and comparable to the reference drugs Ketoconazole and Pentamidine.

## ACKNOWLEDGEMENT

This work has been supported by the Belgian Development Cooperation through VLIR-UOS (Flemish Interuniversity Council - University Cooperation for Development) in the context of the Institutional University Cooperation Programme (IUC) with Universidad de Oriente, Santiago de Cuba, Cuba that started in 2013.

## REFERENCES

Alam MM, Joh EH, Kim Y, Oh YI, Hong J, Kim B, Kim DH, Lee YS. Synthesis and biological evaluation of cyclopentane-linked alkyl phosphocholines as potential anticancer agents that act by inhibiting Akt phosphorylation. J Med Chem, 2011; 47:485-492.

Arba M, Ihsan S, La Ode Ahmad Nur Ramadhan, Tjahjono DH, In silico study of porphyrin-anthraquinone hybrids as CDK2 inhibitor. Comput Biol & Chem, 2017; 67:9–14.

Arboleda M, Jaramilio L, Ortiz D, Diaz A. Leishmaniasis cutánea y herpes zoster multidermatómico. Rev Chil Infectol, 2013; 30: 680–682.

Baiocco P, Colotti G, Franceschini S, Ilari A. Molecular Basis of Antimony Treatment in Leishmaniasis, J Med Chem, 2009; 52:2603-2612.

Barrett MP, Coombs GH, Mottram JC. Recent advances in identifying and validating drug targets in trypanosomes and leishmanias. Trends in microbiology, 1999; 7:82-88.

Bernal FA, Coy-Barrera E. In-Silico Analyses of Sesquiterpene-Related Compounds on Selected Leishmania Enzyme-Based Targets. Molecules, 2014; 19:5550-5569.

Chang LL, Sidler KL, Cascieri MA, de Laszlo S, Koch G, Li B, MacCoss M, Mantlo N, O'Keefe S, Pang M, Rolando A, Hagmann WK. Substituted Imidazoles as Glucagon Receptor Antagonist. Bioorg Med Chem Lett, 2001; 11:2549-2553.

Chauhan PMS, Sunduru N, Sharma M. Recent advances in the design and synthesis of heterocycles as anti-tubercular agents. Future Med Chem, 2010; 2:1469-1500.

dos Reis MB, Manjolin LC, Maquiaveli Cdo C, Santos-Filho OA, da Silva ER. Inhibition of Leishmania (Leishmania) amazonensis and Rat Arginases by Green Tea EGCG, (+)-Catechin and (-)-Epicatechin: A Comparative Structural Analysis of Enzyme-Inhibitor Interactions. PLoS One, 2013; 8:e78387.

Evans DA. History of the Harvard ChemDraw Project. Angew Chem Int Ed, 2014; 53:11140-11145.

Fyfe PK, Oza SL, Fairlamb AH, Hunter WN. Leishmania Trypanothione Synthetase-Amidase Structure Reveals a Basis for Regulation of Conflicting Synthetic and Hydrolytic Activities. J Biol Chem, 2008; 283:17672-17680.

Gasteiger J, Marsili M. Iterative partial equalization of orbital electronegativity a rapid access to atomic charges. Tetrahedron, 1980; 36:3219-3228.

Gharib A, Hashemipour Khorasani BRh, Jahangir M, Roshani M, Bakhtiari L, Mohadeszadeh S. Synthesis of 2,4,5-trisubstituted and 1,2,4,5-tetrasubstituted-1H-imidazole derivatives and or 2,4,5-Triaryloxazoles using of Silica-Supported Preyssler Nanoparticles. Bulg Chem Comm, 2014; 46:165-174.

Gundampati RK, Jagannadham MV. Molecular docking based inhibition of trypanothione reductase activity by taxifolin novel target for antileishmanial activity. J App Pharm Sci, 2012; 2:133-136.

Gundampati RK, Chandrasekaran S, Jagannadham MV. Molecular docking study on the interaction between trypanothione reductase and mangiferin for antileishmanial activity. Bangladesh J Pharmacol, 2013; 8:40-43.

Handman E, Papenfuss AT, Speed TP, Goding JW. 2007. Leishmania Surface Proteins. In: Myler PJ, Fasel N, Ed. Leishmania: After the Genome, Norfolk, UK: Caister Academic Press 177-200.

Jebran AF, Schleicher U, Steiner R, Wentker P, Mahfuz F, Stahl HC, Amin FM, Bogdan C, Stahl KW. Rapid healing of cutaneous Leishmaniasis by high-frequency electrocauterization and hydrogel wound care with or without DAC N-055: A randomized controlled phase II a trial in Kabul. PLoS Negl Trop Dis, 2014; 8:e2694.

Kanyo ZF, Scolnick LR, Ash DE, Christianson DW. Structure of a unique binuclear manganese cluster in arginase. Nature, 1996; 383:554-557.

King AJ, Patrick DR, Batorsky RS, Ho ML, Do HT, Zhang SY, Kumar R, Rusnak DW, Takle AK, Wilson DM, Hugger E, Wang L, Karreth F, Lougheed JC, Lee J, Chau D, Stout TJ, May EW, Rominger CM, Schaber MD, Luo L, Lakdawala AS, Adams JL, Contractor RG, Smalley KS, Herlyn M, Morrissey MM, Tuveson DA, Huang PS. Demonstration of a genetic therapeutic index for tumors expressing oncogenic BRAF by the kinase inhibitor SB-590885. Cancer Res, 2006; 66:11100-11105.

Kumar S, Boehm J, Lee JC. p38 MAP kinases: key signalling molecules as therapeutic targets for inflammatory diseases. Nat Rev Drug Disc, 2003; 2:717-226.

Kumar YC, Malviya M, Chandra JN, Sadashiva CT, Kumar CS, Prasad SB, Prasanna DS, Subhash MN, Rangappa KS. Effect of novel N-aryl urea substituted 3-morpholino arecoline derivatives as muscarinic receptor 1 agonists in Alzheimer's dementia models. Bioorg Med Chem, 2008; 16:5157-5163.

Lambardino JG, Wiseman EH. Preparation and anti-inflammatory activity of some nonacidic trisubstituted imidazoles. J Med Chem, 1974; 17:1182-1188.

Laufer S, Koch P. Towards the improvement of the synthesis of novel 4(5)-aryl-5(4)-heteroaryl-2-thio-substituted imidazoles and their p38 MAP kinase inhibitory activity. Org Biomol Chem, 2008; 6: 437-439.

Loría-Cervera EN, Andrade-Narváez FJ. Animal models for the study of leishmaniasis immunology. Rev Inst Med Trop Sao Paulo, 2014; 56: 1-11.

Manal M, Arul K, Anjana AK, Remya K. Synthesis, docking studies and pharmacological evaluation of imidazole analogues of arecoline. Int J Curr Pharm Res, 2014; 6:22-26.

Palkowitz AD, Steinberg MI, Thrasher KJ, Reel JK, Hauser KL, Zimmerman KM, Wiest SA, Whitesitt CA, Simon RL. Structural Evolution and Pharmacology of a Novel Series of Triacid Angiotensin II Receptor Antagonists. J Med Chem, 1994; 37:4508-4521.

Peitsch MC, Schwede T. Automated protein modeling the proteome in 3D. Pharmacogenomics, 2000; 1:257-266.

Reithinger R, Dujardin JC, Louzir H, Pirmez C, Alexander B, Brooker S. Cutaneous leishmaniasis. Lancet Infect Dis, 2007; 7:581–596.

Rodrigues RF, Castro-Pinto D, Echevarria A, dos Reis CM, Del Cistia CN, Sant'Anna CMR, Teixeira F, Castro H, Canto-Cavalheiro M, Leon LL, Tomás A. Investigation of trypanothione reductase inhibitory activity by 1,3,4-thiadiazolium-2-aminide derivatives and molecular docking studies. Bioorg Med Chem, 2012; 20:1760-1766.

Safari J, Gandomi-Ravandi S, Naseh S. Efficient, green and solvent-free synthesis of tetrasubstituted imidazoles using SbCl3/SiO2 as heterogeneous catalyst. J Chem Sci, 2013; 125:827-833.

Sanner MF. Python: A Programming Language for Software Integration and Development. J Mol Graphics Mod, 1999; 17:57-61.

Sharma D, Narasimhan B, Kumar P, Judge V, Narang R, De Clercq E, Balzarini J. Synthesis, antimicrobial and antiviral evaluation of substituted imidazole derivatives. Eur J Med Chem 2009; 44:2347-2353.

Shin H, Cama E, Christianson DW. Design of Amino Acid Aldehydes as Transition-State Analogue Inhibitors of Arginase. J Am Chem Soc, 2004; 126:10278-10284.

Speck Planche A, Kleandrova VV, Rojas-Vargas JA. QSAR model toward the rational design of new agrochemical fungicides with a defined resistance risk using substructural descriptors. Mol Divers, 2011; 15:901-909.

Sundar S, Rai M. Advances in the treatment of leishmaniasis. Curr Opin Infect Dis, 2002; 15:593–598.

Takle AK, Brown MJ, Davies S, Dean DK, Francis G, Gaiba A, Hird AW, King FD, Lovell PJ, Naylor A, Reith AD, Steadman JG, Wilson DM. The identification of potent and selective imidazole-based inhibitors of B-Raf kinase, Bioorg Med Chem Lett, 2006; 16:378-381.

Tempone AG, Treiger Borborema SE, de Andrade Jr HF, de Amorim Gualda HF, Yogi A, Salerno Carvalho C, Bachiega D, Lupo FN, Bonotto SV, Fischer DCH. Antiprotozoal activity of Brazilian plant extracts from isoquinoline alkaloid-producing families. Phytomedicine, 2005; 12:382–390.

Trujillo I, Kiefer JR, Huang W, Thorarensen A, Xing L, Caspers NL, Day JE, Mathis KJ, Kretzmer KK, Reitz BA, Weinberg RA, Stegeman RA, Wrightstone A, Christine L, Compton R, Li X. 2-(6-Phenyl-1H-indazol-3-yl)-1H-benzo[d]imidazoles: design and synthesis of a potent and isoform selective PKC-zeta inhibitor. Bioorg Lett, 2009; 19: 908-911.

Wallace AC, Laskowski RA, Thornton JM. LIGPLOT: a program to generate schematic diagrams of protein-ligand interactions. Protein Eng, 1996; 8:127-134.

Wishart DS, Knox C, Guo AC, Shrivastava S, Hassanali M, Stothard P, Chang Z, Woolsey J. DrugBank: a comprehensive resource for in silico drug discovery and exploration. Nucleic Acids Res, 2006; 34:D668–D672.

Zampieri D. 2-aryl-3-(1H-azol-1-yl)-1H-indole derivatives: a new class of antimycobacterial compounds - conventional heating in comparison with MW-assisted synthesis. Arch Pharm, 2009; 342:716-722.

**How to cite this article:**
Vargas JAR, Lopez AG, Froeyen M, Piñol MC. Molecular docking study on the interaction between 2-substituted-4,5-difuryl Imidazoles with different Protein Target for antileishmanial activity. J App Pharm Sci, 2018; 8(03): 014-022.